Journal of Cerebral Blood Flow and Metabolism
14:453–465 © 1994 The International Society of Cerebral Blood Flow and Metabolism
Published by Raven Press, Ltd., New York

SPECT Quantification of [^{123}I]Iomazenil Binding to Benzodiazepine Receptors in Nonhuman Primates: II. Equilibrium Analysis of Constant Infusion Experiments and Correlation with In Vitro Parameters

Marc Laruelle, Anissa Abi-Dargham, Mohammed S. Al-Tikriti, Ronald M. Baldwin, Yolanda Zea-Ponce, Sami S. Zoghbi, Dennis S. Charney, Paul B. Hoffer, and Robert B. Innis

Departments of Psychiatry and Diagnostic Radiology, Yale University School of Medicine, New Haven, Connecticut and West Haven VA Medical Center, West Haven, Connecticut, U.S.A.

Summary: In vivo benzodiazepine receptor equilibrium dissociation constant, K_D, and maximum number of binding sites, B_{max}, were measured by single photon emission computerized tomography (SPECT) in three baboons. Animals were injected with a bolus followed by a constant i.v. infusion of the high affinity benzodiazepine ligand [^{123}I]iomazenil. Plasma steady-state concentration and receptor–ligand equilibrium were reached within 2 and 3 h, respectively, and were sustained for the duration (4–9 h) of the experiments (n = 15). At the end of the experiments, a receptor saturating dose of flumazenil (0.2 mg/kg) was injected to measure nondisplaceable activity. Experiments were carried out at various levels of specific activity, and Scatchard analysis was performed for derivation of the K_D (0.59 ± 0.09 n*M*) and B_{max} (from 126 n*M* in the occipital region to 68 n*M* in the striatum). Two animals were killed and [^{125}I]iomazenil B_{max} and K_D were measured at 22 and 37°C on occipital homogenate membranes. In vitro values of B_{max} (114 ± 33 n*M*) and 37°C K_D (0.66 ± 0.16 n*M*) were in good agreement with in vivo values measured by SPECT. This study demonstrates that SPECT can be used to quantify central neuroreceptors density and affinity. **Key Words:** SPECT—Benzodiazepine receptors—Equilibrium—Steady state—[^{123}I]iomazenil.

Single photon emission computerized tomography (SPECT) has been traditionally considered a semiquantitative technique, allowing visualization but not quantification of neuroreceptors. Data analysis has generally been restricted to empirical methods such as region of interest (ROI) counts ratio or ROI washout rates. As these empirical methods do not control for factors such as peripheral clearance, binding to plasma proteins, cerebral blood flow, and regional nonspecific binding, the ability of these measures to provide information about receptor density and affinity is questionable.

To test the ability of SPECT to provide quantitative information about the density and affinity of central neuroreceptors, we performed SPECT experiments with [^{123}I]iomazenil, a probe for the central benzodiazepine receptor (Beer et al., 1990; Innis et al., 1991*a*), in three baboons (*Papio anubis*). In the companion article published in this issue (Laruelle et al. 1994), we described the derivation of benzodiazepine receptor binding potential (BP), i.e., B_{max}/K_D, (Mintun et al., 1984) by compartmental kinetic analysis of [^{123}I]iomazenil brain uptake after single bolus injection in three baboons. In the absence of any information about nonspecific binding (10–20% of total binding), only the total distribution volume, V_T, could be reliably derived by ki-

Received June 14, 1993; final revision received November 1, 1993; accepted November 23, 1993.

Address correspondence and reprint requests to Dr. Marc Laruelle at Department of Psychiatry, Yale School of Medicine, West Haven VA Medical Center/116A2, West Haven, CT 06516, U.S.A.

Abbreviations used: ANOVA, analysis of variance; BP, binding potential; β-CIT, methyl 3β-(4-iodophenyl)tropane-2β-carboxylate; CSF, cerebrospinal fluid; HPLC, high-performance liquid chromatography; PET, positron emission tomography; ROI, region of interest; SA, specific activity; SPECT, single photon emission computerized tomography.

netic analysis. Furthermore, lengthy experiments were needed to derive stable outcome measures (300 min in baboons, 120 min in humans).

Because of the problems associated with kinetic analysis of single bolus experiments, we implemented an alternative paradigm based on constant infusion of the radiotracer. This paradigm creates and maintains a prolonged state of equilibrium at the level of the receptors, allowing direct measurement of V_T (Frey et al., 1985; Kawai et al., 1991; Carson et al., 1992). Injection of receptor saturating doses of a cold competitor allows for measurement of the equilibrium volume of distribution of nonspecific binding during the same experiment.

We previously reported determination of in vivo occipital benzodiazepine receptor B_{max} and K_D in one animal using infusion of high and low specific activity (SA) [^{123}I]iomazenil (Laruelle et al., 1993*a*). In the studies reported here, we extended this approach to various brain regions and performed these experiments in the three animals previously studied using kinetic analysis of single bolus experiments. In addition, we performed studies at five levels of receptor occupancy to confirm the assumption of linearity of the Scatchard plot used to analyze the data. Cerebrospinal fluid (CSF) measurement of [^{123}I]iomazenil was obtained in one animal to validate the assumption that, under prolonged plasma and brain steady state, the intracerebral free tracer equilibrates with the plasma free tracer. Intracerebral radiometabolites were measured after prolonged exposure of the brain to high levels of peripheral radiometabolites.

At the end of these experiments, two of the three baboons were killed. In vitro B_{max}, K_D, and molecular association and dissociation rate constants (k_{on} and k_{off}, respectively) were compared with their in vivo values as derived by SPECT experiments.

METHODS

Radiolabeling

[^{123}I]iomazenil and [^{125}I]iomazenil were labeled as previously described (Zea-Ponce et al., 1993). As the construction of the Scatchard plots required an exact knowledge of SA, [^{123}I]iomazenil preparations were obtained at the desired SA, from high (2,000 Ci/mmol) to low (16 Ci/mmol) SA, by adding unlabeled iomazenil. For [^{125}I]-iomazenil, SA was estimated by ultraviolet (UV) detection at 1,087 Ci/mmol on the day of the labeling. The same batch was used in all in vitro experiments reported here. For both in vivo and in vitro experiments, SA was decay-corrected for time of injection or day of experiment, respectively.

SPECT protocol

SPECT scanning experiments (n = 14) were performed in three female baboons (*Papio anubis*), weighing 10–12 kg, according to protocols approved by the local animal care committee. Identification numbers of each baboon (1, 2, and 3) were the same as those used in the companion paper. At the end of these studies, baboons 2 and 3 were killed. Brains were removed and dissected immediately. Tissue samples were frozen within 120 min of death.

Animal preparation, isoflurane anesthesia, and arterial sampling procedures were identical to those described in the companion paper. Radiotracer was administered as a bolus (30 s), immediately followed by a constant infusion for the entire duration of the experiments. Constant infusion was accomplished through a computer-controlled pump (IMED pump, Jemini PC-1, San Diego, CA, U.S.A.). Experiments lasted 240–540 min, with an average duration of 410 ± 102 min (with these and subsequent values expressed as mean ± SD); duration varied according to estimated time needed to reach equilibrium, which was significantly longer when using a tracer infusion of high as opposed to low SA.

Two experiments at high (2,000 Ci/mmol) SA and one experiment at low (16 Ci/mmol) SA were performed on each animal. In addition, experiments at 77 Ci/mmol (n = 1), 47 Ci/mmol (n = 1), and 25 Ci/mmol (n = 3) were performed on baboon 1.

Average bolus activity was 2.59 ± 0.67 mCi. Average rate of infusion was 0.59 ± 0.19 mCi/h. Average bolus to hourly infusion ratio, B/I, was 4.63 ± 1.56 h. For high (2,000 Ci/mmol) SA experiments (n = 6), the optimal B/I ratio was calculated by computer simulations for each animal, based on the parameters of the peripheral clearance and the brain rate constants derived from single bolus experiment (see Laruelle et al., 1994). Average B/I ratios for high SA experiments were 5.81 ± 1.05 h. Lower B/I ratios were used for low SA experiments (3.75 ± 1.27 h, n = 8). Total injected activity, decay-corrected for the beginning of the experiment, was 6.6 ± 1.8 mCi. A receptor-saturating dose of flumazenil (0.2 mg/kg) was injected as an i.v. bolus 45 min before the end of the infusion to measure the equilibrium nondisplaceable activity. Arterial samples were analyzed as previously described (Zoghbi et al., 1992).

Data were acquired with the CERASPECT camera (Digital Scintigraphics, Cambridge, MA, U.S.A.) (Holman et al., 1990) in continuous mode for 3 min throughout the experiments. Images were reconstructed as described (Laruelle et al., 1994). Activity concentrations were transformed in n*M* using the SA at the time of the beginning of the experiments.

Analysis of in vivo data

The time activity curve of the arterial free parent compound, $f_1C_a(t)$, was fitted to

$$f_1C_a(t) = \sum_{i=1}^{3} C_{0_i}e^{-\lambda_i t} + C_{SS}\sum_{i=1}^{3} f_{0_i}(1 - e^{-\lambda_i t}) \quad (1)$$

where $C_a(t)$ is the arterial concentration of the parent compound (n*M*), f_1 is the free fraction of the tracer in the plasma, C_{0_i} is the zero-time intercept of each exponential (n*M*), λ_i is the elimination rate constant associated with each exponential (min^{-1}), f_{0_i} is the fraction of zero-time intercept associated with each exponential, and C_{SS} (n*M*) is the free concentration at steady state. The first term of

Eq. 1 represents the activity due to the bolus and the second term the activity due to the constant infusion. C_{SS} is related to the clearance, C_L, (L/h), and the rate of infusion, R_o, (nmol/h), by

$$C_{SS} = R_o/C_L \quad (2)$$

From Eq. 1, it is apparent that, in the absence of bolus ($C_0 = 0$), the time to reach steady state is determined by the smallest exponent (λ_3), i.e. the terminal half-life ($\ln(2)/\lambda_3$, 120 ± 39 min, see Laruelle et al., 1994). Ninety percent of C_{SS} is reached after 3.3 half lives (3.3 × 120 min = 396 min). This time can be reduced if a bolus injection is given just prior to the beginning of the constant infusion.

A three-compartment configuration was used to analyze these experiments. This model includes the arterial compartment concentration, C_a, the intracerebral nondisplaceable compartment concentration, C_2, in which the tracer can be free or nonspecifically bound, and the specifically bound compartment concentration, C_3.

The equilibrium volume of distribution, V_i, (ml/g), of a compartment i was defined as the ratio of the tracer concentration in this compartment to the free tracer in the arterial plasma at equilibrium ($V_i = C_i/f_1C_a$) (Carson et al., 1992). V_T is the tissue equilibrium volume of distribution, equal to the sum of V_2 and V_3, the equilibrium volumes of distribution of the nondisplaceable and receptor compartments, respectively.

When equilibrium is reached at the level of the receptors, the Michaelis-Menten receptor-ligand equilibrium equation

$$\text{Bound} = \frac{B_{max}\,\text{free}}{K_D + \text{free}} \quad (3)$$

is satisfied. At tracer doses (free <<< K_D)

$$\frac{\text{Bound}}{\text{free}} = \frac{B_{max}}{K_D} = BP \quad (4)$$

yielding the equivalence between BP and V_3.

The contribution of the activity present in the vasculature in an ROI was estimated assuming a blood volume equal to 5% of the ROI volume (Mintun et al., 1984) and subtracted from the activity concentration in the ROI at time t, $C_{ROI}(t)$, prior to analysis. Thus, $C_{ROI}(t)$ is given by

$$C_{ROI}(t) = C_2(t) + C_3(t) \quad (5)$$

and

$$V_T = \frac{C_{ROI}}{f_1C_a} = V_2 + BP \quad (6)$$

At equilibrium, V_T was directly obtained by the ratio of the brain activity (average value of the last 60 min before flumazenil injection) to the plasma free activity (average plasma activity measured during the same period). V_2 was obtained by the ratio of nondisplaceable activity (activity remaining after flumazenil injection, measured from 20–40 min postinjection) to plasma free activity at that time. BP, as derived with the equilibrium method, BPe, was calculated as the difference between V_T and V_2. High SA constant infusion experiments were also analyzed with a kinetic three-compartment modeling (Mintun et al., 1984; Logan et al., 1987; Frost et al., 1989; Koeppe et al., 1991)

The BP derived by kinetic analysis, BPk, was calculated from kinetic parameters according to

$$BP = \frac{K_1k_3}{k_2k_4f_1} \quad (7)$$

where K_1 and k_2 describe the transfer of tracer across the blood brain barrier and k_3 and k_4 the association and dissociations, respectively, of the tracer-receptor complex.

For derivation of B_{max} and K_D, data from high and low SA experiments were analyzed by Scatchard transformation (Scatchard, 1949) by plotting

$$\frac{\text{Bound}}{\text{free}} = \frac{B_{max}}{K_D} - \frac{\text{Bound}}{K_D} \quad (8)$$

The linear regression of this plot gave the B_{max} (x-axis intercept), the BP (y-axis intercept), and the K_D (negative inverse of the slope). K_D and B_{max} were expressed as nM.

Ex vivo experiment

Baboon 2 was killed by phenobarbital overdose after 500 min of constant infusion (2.17 mCi/h, SA = 2,000 Ci/mmol) preceded by a bolus of 9.2 mCi. Before killing, arterial blood (1 ml), venous blood (2 ml), CSF (6.6 ml), and urine (50 ml) samples were obtained. Fluid samples were analyzed for metabolites as described for plasma samples (see Laruelle et al., 1994). For tissue samples (occipital cortex, striatum, white matter, and cerebellum), 0.2–0.5 g of tissue was homogenized with 2.5 ml 0.9% NaCl while cooling on ice (Brinkmann Polytron, setting 7, 30 s). A 1-ml aliquot of the suspension (containing 2,000–150,000 cpm) was extracted with 3 × 1 ml ethyl acetate and the extract analyzed by HPLC as described for plasma. To correct for recovery of the tracer from the sample matrix, an excess (10 μl, 700,000 cpm) of [^{123}I]-iomazenil was added to a second aliquot of suspension and the mixture analyzed in the same way. Control extraction data were used to correct the experimental sample extraction, as previously described (Zoghbi et al., 1992). CSF and plasma samples were analyzed for protein-bound radioactivity and concentration of free parent compound, as described for plasma samples (see Laruelle et al., 1994). Additional brain samples were collected and frozen at −70°C for homogenate binding studies.

In vitro binding studies

In vitro assays were performed on occipital samples obtained from baboons 2 and 3 and from one additional animal (baboon 4), whose brain was obtained under conditions similar to the others. In vitro assays were performed at least 60 days after killing in order, to allow complete decay of [^{123}I]iomazenil. On the day of the assay, brain samples were weighed, thawed, and homogenized with a Polytron (setting 6 for 10 s) in 1/400 (wt/vol) wet weight (in mg)/vol (in ml) of buffer (25 mM KPO_4, 150 mM NaCl, pH 7.4). After homogenization, tissues were centrifuged (20,000g, 4°C, 10 min). Supernatant was discarded and pellets resuspended and recentrifuged. This procedure was repeated twice.

Incubation was initiated by the successive addition of 100 μl of [^{125}I]iomazenil, 100 μl buffer or unlabeled iomazenil, and 800 μl of tissue solution. A final tissue dilution of 1/2,400 (wt/vol) was selected so that total binding was between 5 and 10% of total ligand concentration. Incuba-

tion was terminated by rapid filtration though GF/B filters on a 48-channel Cell Harvester (Brandel, Gaithersburg, MD, U.S.A.). Filters were washed rapidly three times with 5 ml ice-cold buffer and counted in a COBRA 5010 gamma counter (Packard, Meriden, CT, U.S.A.) with an efficiency of 80%.

Saturation experiments (n = 5–6) were performed by the isotopic dilution method ("cold" saturation) at 22 and 37°C on baboons 2, 3, and 4, using a single concentration of [^{125}I]iomazenil (0.02 n*M*) and fifteen concentrations of nonradioactive iomazenil (10^{-14}–10^{-6} *M*). Incubation time was 45 min at 22°C and 30 min at 37°C. Each concentration was performed in triplicate.

Kinetic experiments were performed on baboon 2. Association experiments (n = 3) were performed at 22 and 37°C at four and three [^{125}I]iomazenil concentrations, respectively, for 12 time periods ranging from 1 to 90 min. Nonspecific binding was measured as the binding remaining in the presence of 1 μ*M* iomazenil at 4, 20, and 40 min. Dissociation experiments (n = 3) were performed after preincubation of tissue with 0.02 n*M* [^{125}I]iomazenil for 45 min at 22°C and 30 min at 37°C. Dissociation was initiated by the addition of 1 μ*M* iomazenil and terminated at 14 different times ranging from 1 to 120 min. Nonspecific binding was measured with 1 μ*M* iomazenil added at the beginning of the preincubation.

Analysis of in vitro data

Saturation experiments were analyzed by nonlinear regression analysis using the program LIGAND (Munson and Rodbard, 1980; NIH, Bethesda, MD, U.S.A.). A measurement variance increasing as the square of the values was assumed and the least-square criterion adjusted accordingly. Nonspecific binding was estimated by the regression. K_D and B_{max} values were expressed (n*M*).

Association and dissociation experiments were analyzed using the program Kaleidagraph 2.1 (Abelbeck Software, Reading, PA, U.S.A.). For association experiments, nonspecific binding at each time was estimated by linear regression of the three measured nonspecific binding and this value was subtracted from each point to derive the specific binding association curve. This curve was fitted by nonlinear regression to the exponential curve $B_t = B_E(1 - \exp(k_{obs}t)$, where B_t is the specific binding at time t, B_E the specific binding at equilibrium, and k_{obs} is the observed association rate constant (min^{-1}). Specific binding dissociation curves were fit to $B_t = B_E\exp(k_{off}t)$ after subtraction of the nonspecific binding.

Two methods were used to drive k_{on} and K_D. In the first method (ratio method), k_{on} was calculated for each association curve as

$$k_{on} = \frac{k_{obs} - k_{off}}{free} \quad (9)$$

with k_{off} equal to the mean k_{off} of all dissociation experiments performed under similar conditions. In the second (graphical method), values of k_{obs} derived from all association experiments were plotted against values of the free. Values of k_{off} and k_{on} were then calculated by linear regression according to

$$k_{obs} = k_{on}\,free + k_{off} \quad (10)$$

In vitro k_{on} and k_{off} values were compared to regional in vivo k_{on} and k_{off} values derived from the rate constants k_3 ($k_3 = k_{on}B_{max}/V_2$) and k_4 ($k_4 = k_{off}$). For the purpose of this derivation, we used average regional V_2 and B_{max} values measured by equilibrium analysis of constant infusion experiments and average regional rates constant k_3 and k_4 measured by kinetic analysis of single bolus experiments as described (Table 3 of Laruelle et al., 1994).

Statistical analysis

Data variance was tested for statistical significance with general linear modeling analysis of variance (ANOVA). Particular configuration of ANOVA models are indicated in the results section (dependent variable: ANOVA, factor × factor; p values) with exact p values provided unless $p < 0.01$.

RESULTS

Peripheral clearance and plasma steady state

Plasma-free iomazenil concentration, metabolite-corrected, was essentially stabilized at ~120 min and remained constant for the duration of the experiments (Fig. 1). In contrast, total plasma activity increased with time, reflecting the increasing amount of radiolabeled metabolites.

Clearance and C_{SS} were calculated by fitting the arterial free parent compound concentration to Eq. 1 (Table 1). The clearance calculated by the ratio of free concentration at time of measurement (n*M*) to the infusion rate in nmol/h, Eq. 2, was 34.4 ± 19 L/h, a value very close to the clearance derived from the fit (35.6 ± 17 L/h). As observed in single bolus experiments (see Laruelle et al., 1994, Table 2), the clearance of baboon 1 (45.9 ± 17 L/h, n = 8) was significantly faster than those of baboons 2 (19.5 ± 2.11 L/h, n = 3) and 3 (24.0 ± 3.6 L/h, n = 3) (ANOVA, $p = 0.025$).

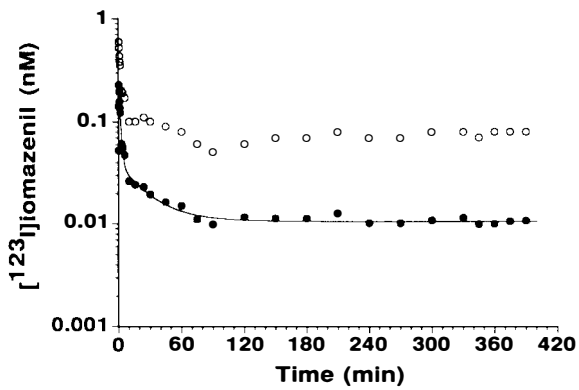

FIG. 1. Arterial total activity (open circles) and free parent [^{123}I]iomazenil (closed circles) during constant infusion of 0.54 mCi/h in baboon 3. The constant infusion was preceded by a bolus injection of 2.70 mCi (bolus to hourly infusion ratio of 5.03 h). The total administered dose was 6.19 mCi. Free parent concentration reached a steady state level within 120 min. Measured values (points) were fitted to Eq. 1 (solid line). Plasma kinetic parameters were used to calculate the clearance (24 L/h). The fitted C_{SS} concentration was 0.105 n*M*.

TABLE 1. *[^{123}I]iomazenil peripheral clearance during constant infusion*

Baboon	n	f_1[a]	V_{bol}[a] (L)	CL[a,b] (L/h)	Terminal[a,b] half-life (min^{-1})
B1	8	0.318 ± 0.037	5.8 ± 0.9	46 ± 17.3	105 ± 31
B2	3	0.350 ± 0.019	6.1 ± 0.9	19.5 ± 2.1	169 ± 37
B3	3	0.354 ± 0.023	6.6 ± 0.7	24 ± 3.7	183 ± 57
Mean ± SD	14	0.332 ± 0.034	6 ± 0.9	35.6 ± 17.9	135 ± 51

[a] Values are mean ± SD.
[b] Statistically different ($p < 0.01$) between animals.

For each experiment, we expressed the measured plasma free concentrations (f_1C_a) at different time points as a percentage of the fitted C_{SS} values. At 60 min, plasma values were 126 ± 13% of C_{SS} and decreased asymptotically with time, reaching 101 ± 1% at 600 min. At the time of measurement of V_T (360 ± 90 min), measured values of arterial free tracer concentration had reached 105 ± 9% of C_{SS}.

High SA experiments

Regional brain [^{123}I]iomazenil concentration displayed stable levels within 180 min and until the injection of flumazenil, indicating that a state of equilibrium was reached and maintained (Fig. 2). Average ROI concentrations for each hour postinjection were calculated for the high SA experiments (n = 6) and expressed as % of the activity during the 60 min preceding the flumazenil injection (Table 2). The flumazenil injection induced a rapid displacement (within 30 min) of the brain activity (Fig. 2). The average [^{123}I]iomazenil concentration between 20 and 40 min after flumazenil injection represented only 10–14% of the concentration prior to injection (Table 2).

Since stable levels of [^{123}I]iomazenil concentration were observed in both the brain and the arterial plasma during the 60 min prior to flumazenil injection, this period was selected for measurement of V_T. As brain concentration was stable from 20–40 min post flumazenil injection, this period was selected to calculate V_2. The rank order of average regional values of BPe (occipital, 238 ± 5; temporal, 164 ± 6; frontal, 150 ± 3; thalamus, 113 ± 11; striatum, 107 ± 11) (Table 3) was in accordance with the distribution of benzodiazepine receptors as measured by autoradiography in primate brain (Sybirska et al., 1992). Differences in V_T, V_2, and BPe between regions and baboons were investigated by ANOVA. No statistically significant differences between baboons were noted. Regional differences were significant for V_T (ANOVA; region × baboon; region, $p < 0.01$; baboon, $p = 0.55$) but not for V_2 (ANOVA; region × baboon; region, $p = 0.28$; baboon, $p = 0.64$).

Three-compartment kinetic analysis was also performed on these data (Table 4). Since a measured V_2 value was available for each region, the K_1/k_2 ratio was constrained to V_2f_1. K_1 ranged from 0.644 ± 0.202 ml g^{-1} min^{-1} (striatum) to 1.057 ± 0.339 ml g^{-1} min^{-1} (occipital), with high %CV (from 7 ± 4% in occipital to 27 ± 16% in frontal). Values of k_3 (from 0.386 ± 0.281 min^{-1} in occipital to 0.122 ± 0.117 min^{-1} in striatum) and k_4 (from 0.0227 ± 0.074 min^{-1} in frontal to 0.0631 ± 0.0246 min^{-1} in thalamus) were affected by a high %CV (49–121% for k_3, 49–64% for k_4) and poorly identified. The kinetic BP (BPk), derived from the ratio of these rate constants (Eq. 7), was very close to the BPe measured in each region (Table 3). The average absolute difference between BPe and BPk, expressed as % BPe, was 4.8 ± 3.6%.

The reproducibility of each outcome measure (V_T, V_2, BPe, and BPk) was evaluated by the %CV between the test and retest (Table 5). The overall %CV (all regions) was 9 ± 1% for V_T, 19 ± 11% for V_2, 8 ± 2% for BPe, and 5 ± 2% for BPk. Differences in outcome measure reproducibility between regions and animals were investigated by ANOVA. Reproducibility of the V_2 measurement was significantly worse than other outcome measures ($p < 0.01$). There were no significant differences in reproducibility between regions ($p = 0.40$). Baboon 2 test/retest (47 days) had a significantly lower reproducibility (mean %CV of all outcome measures and

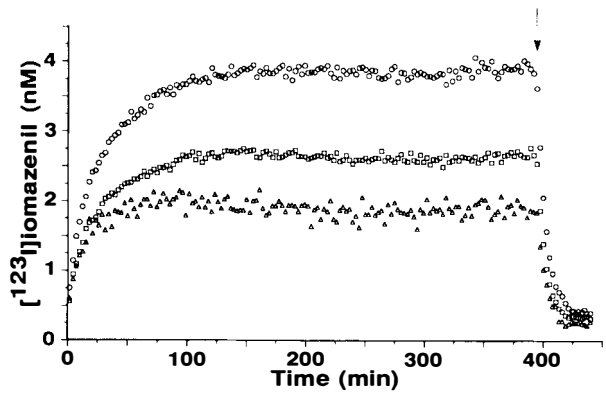

FIG. 2. [^{123}I]iomazenil concentration in occipital (circles), temporal (squares), and striatal (triangles) ROIs during bolus plus constant infusion (bolus = 3.33 mCi, infusion = 0.47 mCi/h, B/I = 7.01) of high SA tracer (2,000 Ci/mmol) in baboon 1. In regions with high receptor density, such as the occipital, equilibrium was reached within 150 min. In regions with low density of receptors, such as the striatum, equilibrium was reached more rapidly (within 80 min). The temporal region displayed an intermediate profile. In all regions, stable activity levels were maintained until the injection of 0.5 mg/kg flumazenil (arrow) at 400 min. Nondisplaceable binding (0.46 n*M* in the occipital) was subtracted from the total (3.85 n*M*) to calculate the specific binding (3.4 n*M*). The specific binding was divided by the arterial free steady state concentration (0.0132 n*M*) to yield the binding potential (256).

TABLE 2. *Regional approach to equilibrium in high SA experiments*

Region	Time (min)[a]						After flumazenil[b] (0.2 mg/kg)
	0–60	60–120	120–180	180–240	240–300	300–360	
Occipital	67 ± 11	91 ± 7	97 ± 5	99 ± 3	100 ± 2	100	10 ± 1
Temporal	71 ± 13	94 ± 8	99 ± 5	100 ± 2	101 ± 2	100	11 ± 3
Frontal	68 ± 14	92 ± 7	98 ± 5	99 ± 4	100 ± 3	100	11 ± 1
Striatum	86 ± 10	102 ± 7	102 ± 5	100 ± 3	100 ± 2	100	14 ± 2
Thalamus	87 ± 12	103 ± 8	102 ± 5	100 ± 2	100 ± 1.8	100	14 ± 3

[a] Values are means ± SD of ROI activity (n = 6), averaged for 60 min (15 acquisitions), expressed as % of the 300–360 min activity.
[b] Values after flumazenil injection are average values from 15 to 45 min after i.v. bolus injection of a receptor saturating dose (0.2 mg/kg) of nonradioactive flumazenil.

all areas 15 ± 14%, n = 20) than did baboons 1 (21 days; 9 ± 7%) and 3 (13 days; 7 ± 5%, $p = 0.021$).

Low SA experiments

At low SA, brain activity stabilized within the first hour. V_T, V_2, and B/F were calculated as for high SA experiments. At the lowest specific activity (16 Ci/mmol), V_2 represented 22 (occipital) to 26% (striatum) of V_T. B_{max} and K_D were derived by Scatchard analysis (Fig. 3, Table 5). B_{max} values were significantly different among regions (ANOVA; $p < 0.01$) but not K_D values ($p = 0.70$). The mean regional K_D was 0.59 ± 0.09 n*M* (n = 15). The coefficient of determination of the regression (r^2) was higher for baboons 2 (average regional r^2, 0.96 ± 0.02) and 3 (0.96 ± 0.04) than for baboon 1 (0.85 ± 0.04; ANOVA, $p < 0.01$), the difference presumably being related to the higher number of points (n = 8) in baboon 1, as compared to baboons 2 and 3 (n = 3). Saturation data from baboon 1 were also analyzed with the nonlinear regression program LIGAND (Munson and Rodbard, 1980). The one-site model provided results similar to those of linear regression analysis of Scatchard plots. A two-site model failed to converge.

Ex vivo experiment

After 500 min of [^{123}I]iomazenil infusion, radiolabeled metabolites were present at negligible levels in gray matter (<1% of activity) (Table 6) and at low levels in white matter (15%) and CSF (24%). In contrast, radiolabeled metabolites represented 71 and 74% of total activity in arterial and venous plasma, respectively; 100% of the urine activity consisted of radiometabolites.

In CSF, the parent compound was essentially free (free fraction = 0.927). Free CSF parent compound concentration (0.046 n*M*) was similar to

TABLE 3. *Reproducibility of equilibrium and kinetic analysis of high SA constant infusion experiments*

Baboon	Region	Test		Retest		Reproducibility	
		BPe	BPk	BPe	BPk	% CV BPe	% CV BPk
1	Occipital	246	233	222	221	7.3	3.7
	Temporal	176	167	165	164	4.5	1.4
	Frontal	162	153	140	139	10.4	7.0
	Striatum	128	120	112	108	9.6	7.4
	Thalamus	122	112	109	106	8.0	4.2
2	Occipital	231	244	257	250	7.4	1.9
	Temporal	155	161	172	164	7.2	1.5
	Frontal	130	135	163	159	15.8	11.8
	Striatum	92	91	105	95	9.3	2.8
	Thalamus	104	104	122	111	11.3	4.5
3	Occipital	234	264	237	244	1.0	5.5
	Temporal	147	164	170	176	9.9	4.8
	Frontal	152	171	151	158	0.7	5.6
	Striatum	94	101	113	112	13.2	7.6
	Thalamus	118	126	106	107	7.4	11.5
Average % CV ±SD						8.2 ± 4.0	5.4 ± 3.2

BPe, equilibrium BP, calculated as the difference between V_T and V_2; BPk, kinetic BP, calculated as $K_1k_3/k_2k_4f_1$; % CV, calculated as 100 (SD of test and retest)/(mean of test and retest).

TABLE 4. *Kinetic analysis of high SA constant infusion experiments*

Region	K_1 (ml/g min)	k_2 (min^{-1})	k_3 (min^{-1})	k_4 (min^{-1})	BPk
Occipital	1.057 ± 0.339	0.141 ± 0.079	0.386 ± 0.281	0.0365 ± 0.0254	243 ± 15
Temporal	0.844 ± 0.258	0.123 ± 0.047	0.332 ± 0.336	0.0370 ± 0.0371	166 ± 5
Frontal	0.689 ± 0.134	0.104 ± 0.044	0.198 ± 0.114	0.0227 ± 0.0074	150 ± 15
Striatum	0.644 ± 0.202	0.083 ± 0.044	0.122 ± 0.117	0.0243 ± 0.0115	93 ± 20
Thalamus	0.670 ± 0.084	0.047 ± 0.007	0.133 ± 0.049	0.0631 ± 0.0246	86 ± 8

Values are means ± SD of six experiments. Parameters were estimated by three compartment fit with K_1/k_2 ratio constrained to $V_2 f_1$, with f_1 measured in plasma and V_2 measured after flumazenil injection. CV% was calculated as 100 (standard error of the parameter as estimated by diagonal of covariance matrix/parameter value).

those of free parent compound in arterial and venous plasma (0.055 and 0.045 n*M*, respectively, Table 7).

In vitro experiments

Saturation experiments. Saturation experiments were performed on the occipital cortices of baboons 2, 3, and 4 at 22 and 37°C (Table 8, Fig. 4). The K_D at 22°C (0.35 ± 0.11 n*M*, n = 16) was significantly lower than the K_D at 37°C (0.66 ± 0.16 n*M*, n = 6; ANOVA, $p < 0.01$), but the B_{max} was similar at 22 (113 ± 35 n*M*, n = 16) and 37°C (116 ± 26 n*M*, n = 6; ANOVA, $p = 0.83$). No significant differences in K_D or B_{max} values were found between the three animals (K_D: ANOVA, $p = 0.53$; B_{max}: ANOVA, $p = 0.65$). The mean B_{max} derived from all assays (n = 22) was 114 ± 33 n*M*. This value compared favorably to the mean B_{max} derived from the in vivo experiments (126 ± 13, n = 3). Of interest is the finding of a lower B_{max} for baboon 2 as compared to baboon 3 both in vitro (108 ± 20 versus 124 ± 30 n*M*) and in vivo (129 versus 137 n*M*). The K_D derived from SPECT experiments (0.54 ± 0.04, n = 3) was somewhat closer to the in vitro K_D measured at 37°C (0.66 ± 0.16 n*M*) than to that measured at 22°C (0.35 ± 0.11 n*M*). A limited number of saturation studies (n = 2) were performed to measure B_{max} in four additional regions (baboon 2: temporal cortex, 100 ± 1 n*M*; frontal cortex, 101 ± 5 n*M*; striatum, 52 ± 4 n*M*; and thalamus, 50 ± 5 n*M*). This site density distribution was in accordance with the distribution of [^{125}I]iomazenil binding in primate brain previously studied by autoradiography (Sybirska et al., 1992). No differences in K_D were observed between regions (data not shown).

TABLE 5. *High and low SA experiments: in vivo regional B_{max} and K_D*

Region	K_D[a] (n*M*)	B_{max}[ab] (n*M*)	r^2[a]
Occipital	0.53 ± 0.04	126 ± 14	0.89 ± 0.06
Temporal	0.56 ± 0.10	92 ± 16	0.90 ± 0.06
Frontal	0.59 ± 0.07	88 ± 13	0.89 ± 0.07
Striatum	0.65 ± 0.10	68 ± 13	0.82 ± 0.53
Thalamus	0.62 ± 0.13	70 ± 15	0.87 ± 0.50
Regional average ±SD	0.59 0.09		

r^2, average regression coefficient of Scatchard plot.

[a] Values are means ± SD of three determinations of K_D and B_{max} by Scatchard analysis (3–8 experiments at various level of SA per Scatchard analysis).

[b] Significantly different across regions (ANOVA, $p = <0.01$).

Kinetic experiments. Results of the ratio (Table 9) and graphical (Fig. 5) analyses were in good agreement. The dissociation was about ten times slower at 22°C, (k_{off} = 0.0301 ± 0.0021 min^{-1}, n = 3, corresponding to a dissociation half time, T_d 0.5, of 22.3 min), than at 37°C (k_{off} = 0.320 ± 0.006 min^{-1}, n = 3, $T_{d\ 0.5}$ of 2.3 min; ANOVA, $p < 0.01$). The association was about four times slower at 22°C (k_{on} = 0.124 ± 0.058 min^{-1} nM^{-1}, n = 3), than at 37°C (k_{on} = 0.364 ± 0.420 min^{-1} nM^{-1}; ANOVA, $p < 0.01$). K_D values calculated from kinetic experiments (0.29 ± 0.11 n*M* at 22°C and 0.84 ± 0.11 n*M* at 37°C) were in excellent agreement with K_D values derived from saturation experiments.

In vivo k_{off} and k_{on} values were calculated using the regional in vivo B_{max} values derived from constant infusion experiments and the regional k_3 and k_4 values derived from kinetic analysis of single bolus experiments, where rate constants were best identified (Table 3, Model B). The in vivo K_D value derived from the in vivo k_{off}/k_{on} ratio (0.62 ± 0.09) was in excellent agreement with that derived by Scatchard analysis (0.59 ± 0.09 n*M*). However, association and dissociation rate constants observed in vivo were significantly slower than those in vitro. Furthermore, in vivo k_{off} values measured at low receptor occupancy were not compatible with the rapid rate of brain washout observed after injection of receptor-saturating doses of flumazenil. For example, in the experiment depicted in Fig. 6, 80% of the tracer washed out with a rate of 0.18 min^{-1}. Given the fact that the delivery and binding of flumazenil is rapid but not instantaneous, this observation suggested that k_{off} should be >0.18 min^{-1}, which is compatible with the 37°C in vitro k_{off} (0.32 min^{-1}) value but not with the in vivo k_{off} value

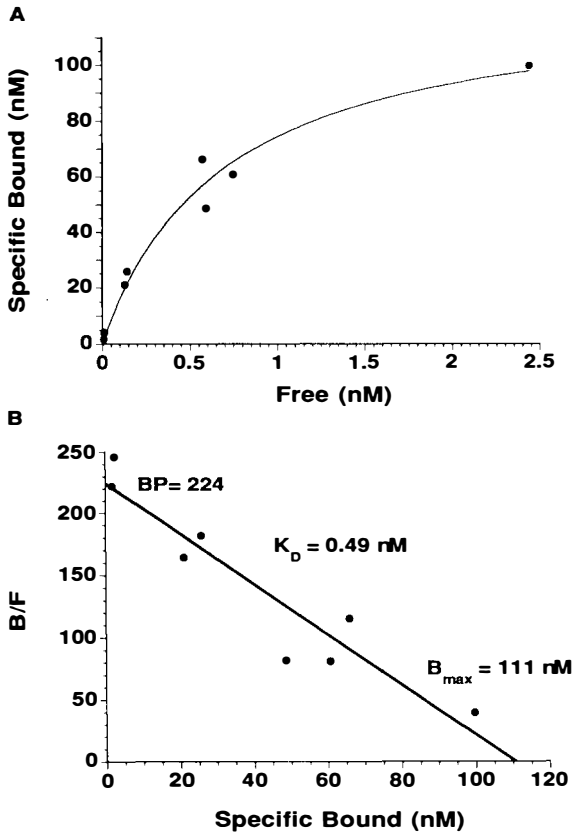

FIG. 3. In vivo determination of occipital K_D and B_{max} (baboon 1). **A:** Equilibrium saturation curve obtained from the data of eight constant infusion experiments with various levels of SA (2,000 Ci/mmol, n = 2; 77 Ci/mmol, n = 1; 47 Ci/mmol, n = 1; 25 Ci/mmol, n = 3; 16 Ci/mmol; n = 1). For each experiment, the arterial, metabolite-corrected, free steady state level of [^{123}I]iomazenil was plotted versus the occipital specifically bound, as calculated by the difference between the pre- and postflumazenil injection occipital equilibrium concentration. **B:** Scatchard transformation. The regression line (r^2 = 0.88) allowed calculation of BP as the *y* axis intercept (224 n*M*), B_{max} as the *x* axis intercept (111 n*M*), and K_D as the inverse of the slope (0.49 n*M*).

calculated in the absence of flumazenil (0.015 min^{-1}).

DISCUSSION

The most significant results of these studies are those demonstrating the feasibility of a constant infusion paradigm to induce and sustain a state of equilibrium at the receptor site, and the excellent agreement between in vivo BP values derived by kinetic and equilibrium methods and between in vivo and in vitro measurement of B_{max} and K_D.

Advantages of the constant infusion paradigm

Multiple advantages are associated with this constant infusion paradigm:

(a) No prior derivation of rate constants. The binding parameters of interest (BP, K_D, and B_{max}) can be calculated independently of the transfer rate constants that are difficult to identify unless some assumptions and/or constraints are implemented in the regression process (see Laruelle et al., 1994). Furthermore, the kinetic model becomes nonlinear and, therefore, more complex at nonnegligible receptor occupancy. That is not the case for the constant infusion/equilibrium paradigm.

(b) Direct measurement of nonspecific binding. This paradigm provides a stable baseline for evaluation of pharmacological challenge tests or dose–receptor occupancy relationship studies (Innis et al., 1991*b*). In addition, this stable baseline allows the direct measurement of the nondisplaceable compartment equilibrium distribution volume (V_2) after flumazenil injection. The estimation of V_2 is problematic in the absence of a region of reference devoid of receptors. In Laruelle et al., 1994 we reported that the estimation of V_2 by an unconstrained three-compartment model was associated with a relatively large error. This induced a lower reproducibility of the BP estimation by the unconstrained three-compartment fit (% CV, mean of all regions = 15%) as compared to a V_2 constrained fit (% CV, mean of all regions = 10%). The direct measurement of V_2 in each region in the studies reported here contributed to an increased reproducibility (% CV, mean of all regions: 8 ± 2%).

(c) Direct measurement of the free tracer concentration. This paradigm avoids the assumptions

TABLE 6. *Relative composition of brain and fluid activity after 500 min [^{123}I]iomazenil infusion*

Tissue	Relative composition[a] Parent compound (%)	Lipophilic metabolite (%)	Polar metabolite (%)
Occipital cortex	99	1	ND
Striatum	100	ND	ND
Cerebellum	99	1	ND
White matter	85	9	6
CSF	76	14	10
Arterial plasma	28	18	54
Venous plasma	25	15	60
Urine	ND	42	58

[a] Values are expressed in % total activity; ND, nondetected.

TABLE 7. *Steady state level of CSF and plasma activity after 500 min [^{123}I]iomazenil infusion*

Fluid	Concentration[a] Parent	Free parent	Free fraction
CSF	0.050	0.046	0.920
Arterial plasma	0.118	0.055	0.466
Venous plasma	0.096	0.045	0.469

[a] Concentration expressed as n*M*.

TABLE 8. *Comparison in vitro and in vivo [^{123}I]iomazenil B_{max} and K_D*[a]

	In vitro								In vivo		
	22°C			37°C			Average				
Baboon	n	K_D	B_{max}	n	K_D[b]	B_{max}	n	B_{max}	n	K_D	B_{max}
1									1	0.49	111
2	5	0.28 ± 0.07	106 ± 25	3	0.61 ± 0.17	110 ± 20	8	108 ± 20	1	0.52	129
3	6	0.36 ± 0.11	125 ± 30	3	0.71 ± 0.16	122 ± 36	9	124 ± 30	1	0.57	137
4	5	0.38 ± 0.14	108 ± 48				5	108 ± 48			
Mean ± SD	16	0.35 ± 0.11	113 ± 35	6	0.66 ± 0.16	116 ± 28	22	114 ± 33	3	0.545 ± 0.04	126 ± 13

[a] All values are mean ± SD and expressed (n*M*).
[b] Statistically significant different from 22°C K_D values (ANOVA, $p < 0.01$).

needed for equilibrium analysis of bolus-only experiments regarding the level of free tracer in the brain at equilibrium. In the equilibrium method developed by Farde et al. (1986) for analysis of [^{11}C]raclopride binding, the total cerebellar activity is used as an estimate of the free (V_2 is assumed to be unity). As acknowledged by the authors (Farde et al., 1989), this assumption is likely to produce an artifactual 10-fold increase of the K_D. Using a constant infusion paradigm, the concentration of free tracer in the brain can be directly estimated by the measurement of free tracer in the blood. The validity of this approach has been confirmed by CSF and microdialysis measurements. Using CSF tracer concentration as a measure of the free intracerebral tracer concentration, Kawai et al. (1991) found a close correlation between CSF and plasma water tracer concentration under constant infusion. Using microdialysis, Dubey et al. (1989) showed that the ratio between intracerebral free concentration of [^{3}H]diazepam and free plasma concentration was equal to unity at equilibrium. In this study, we obtained one CSF sample during [^{123}I]iomazenil constant infusion and found a concentration similar to arterial and venous free tracer concentrations, supporting the validity of this approach for [^{123}I]iomazenil.

(d) Insensitivity to the ratio of peripheral clearance and brain-washout rate. The method developed here is similar to the "transient equilibrium" analysis method used to measure [^{11}C]flumazenil BP (Pappata et al., 1988; Brouillet et al., 1990; Iyo et al., 1991), with the exception that, through the constant infusion, the terminal half life is effectively set to zero. Transient equilibrium analysis method measures the regional volume of distribution when the brain to plasma ratio is constant, i.e., when both concentrations decrease at the same rate. However, Carson et al. (1992) recently demonstrated that this ratio (V_a) is an overestimation of the true equilib-

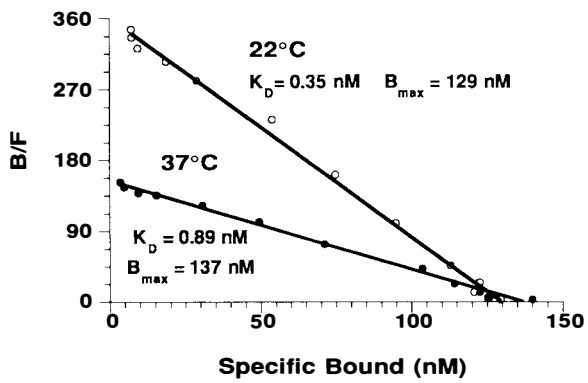

FIG. 4. In vitro Scatchard analysis of saturation experiments performed with [^{125}I]iomazenil (isotopic dilution method) in homogenate membranes from the occipital cortex of baboon 3. Data presented are from a typical experiment, each point representing the mean of three determinations. Temperature affected the affinity but not the B_{max}. The average B_{max}, measured in vitro (124 ± 30 n*M*, n = 9), was in good agreement with the in vivo B_{max} measured in this animal (137 n*M*).

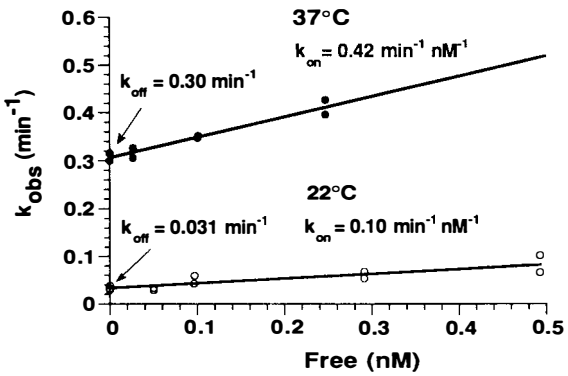

FIG. 5. Graphical analysis of in vitro kinetic association and dissociation experiments performed at 22 and 37°C in homogenate membranes of occipital cortex from baboon 2. Each point on the line represents results of one experiment. Association experiments were performed at various concentrations of [^{125}I]iomazenil (0.02–0.5 n*M*). Dissociation experiments (*y*-axis intercept) were performed at 0.02 n*M*. Linear regression of free versus k_{obs} yielded k_{off} as the *y*-axis intercept and k_{on} as the slope. Ratios of k_{off} to k_{on} yielded K_D values that were in good agreement with K_D values measured with equilibrium saturation experiments. In vitro k_{off} and k_{on} rate constants were considerably higher than in vivo k_{off} (0.015 min^{-1}) and k_{on} (0.0250 min^{-1} nM^{-1}).

TABLE 9. *In vitro and in vivo molecular rates constants*[a]

In vitro								In vivo			
22°C				37°C							
n	k_{off} (min^{-1})	k_{on} ($min^{-1}nM^{-1}$)	K_D (nM)	n	k_{off} (min^{-1})	k_{on} ($min^{-1}nM^{-1}$)	K_D (nM)	n	k_{off} (min^{-1})	k_{on} ($min^{-1}nM^{-1}$)	K_D (nM)
5	0.0301 ± 0.0021	0.124 ± 0.058	0.29 ± 0.11	4	0.320 ± 0.006	0.364 ± 0.053	0.84 ± 0.11	5	0.0249 ± 0.0027	0.0154 ± 0.0013	0.62 ± 0.08

In vitro values were measured on occipital homogenate membranes from baboon 2. In vivo values are average values from five regions, using average in vivo B_{max} and average regional k_3 and k_4 as derived from single bolus experiments in baboons 1, 2, and 3.
[a] Values are mean ± SD.

rium distribution volume by a factor related to the ratio of λ_n, the terminal half-life, to α_1, the smallest eigenvalue of the brain impulse response function, according to the following equation

$$V_a = \frac{V_T}{1 - \lambda_n/\alpha_1}$$

Hence, during constant infusion, $\lambda_n = 0$ and the brain/plasma ratio (V_a) are true measures of V_T.

(e) Insensitivity to blood flow changes during the experiment. Both kinetic and equilibrium analyses of reversible tracers, as opposed to empirical methods, provide blood-flow–independent outcome measures. However, kinetic analysis assumes that blood flow is constant over the course of the experiment. This might not be true, especially in human experiments. In contrast, in the constant infusion paradigm, once plasma steady state and receptor equilibrium have been established, the brain activity concentration is independent of the blood flow.

(f) Suitability for SPECT physics limitations. The constant infusion paradigm appears to be particularly well suited for SPECT experiments. Because of the lower sensitivity of SPECT as compared to positron emission tomography (PET), the minimal acquisition time needed to reach an adequate level of counts is longer for SPECT, limiting implementation of the kinetic method in SPECT experiments. Because the constant infusion method provides a stable level of activity for a prolonged period of time, the acquisition time can be greatly increased, allowing higher counting statistics and resolution, and, as a consequence, lower doses of activity and lower radiation exposure to human subjects.

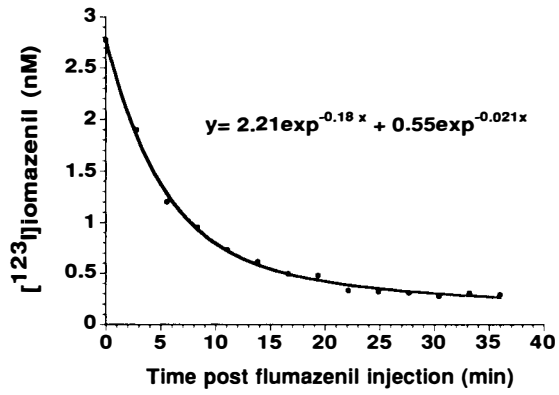

FIG. 6. [^{123}I]iomazenil washout from the occipital cortex (baboon 1) after flumazenil injection (0.2 mg/kg). These data were acquired during a constant infusion experiment (2,000 Ci/mmol), 420 min after initiation of the constant infusion (0.58 mCi/h). The time on the *x*-axis is the time after flumazenil injection. About 80% of the tracer washed out at a rate of 0.18 min^{-1}, which is >10 times faster than the in vivo k_{off}, as measured in kinetic experiments at high SA (0.0154 min^{-1}). This paradox, observed for multiple high affinity ligands, is only poorly elucidated.

(g) Short scanning session. In the studies described in this article, data were acquired throughout the experiment. However, the equilibrium analysis was performed only on data acquired 60 min before flumazenil injection. Using data acquired only 15 min before flumazenil injection yielded similar results (data not shown). Thus, in human studies, data acquisition can be limited to 15 min as compared to single bolus/kinetic analysis experiments, in which a minimal 120-min period of acquisition is needed to derive the BP (unpublished data).

(h) No arterial sampling. In this method, a limited amount of blood sampling is needed to measure the C_{SS} concentration of the tracer, as opposed to the single bolus/kinetic analysis protocol, which requires characterization of the input function for the whole duration of the experiment. In addition, we can assume that, under steady state conditions, arterial and venous tracer concentrations would equilibrate and that no arterial sampling would be needed. This hypothesis will be tested in our experiments in human subjects.

(i) Simple computation procedure. The ability to derive the paradigm of interest without prior derivation of rate constants make the computation procedure much easier. A pixel-by-pixel analysis would, therefore, be easier to implement.

Problems associated with the constant infusion paradigm

Potential problems associated with the use of this method must be noted. If the time spent in the camera can be substantially reduced, the overall duration of the experiments (infusion time) is increased

by two–three-fold, which is not always convenient. Although infrequent, there is a potential for pump failure. Of bigger concern is the fact that, in a reduced version of the protocol (data acquired only at the end of the experiments), it might be difficult to verify that equilibrium has been reached by the time of data acquisition. Several acquisitions might, thus, be needed to establish that equilibrium has been reached.

In the experiments reported here, we used peripheral clearance data obtained in these animals in previous single bolus experiments to optimize the bolus to hourly infusion ratio needed to reach equilibrium rapidly. The use of a common, standard bolus to hourly infusion ratio for each animal would have delayed establishment of the equilibrium in some experiments. In human studies, no a priori knowledge of the clearance would be available. However, preliminary experiments in healthy human subjects (n = 8, unpublished data) showed that a bolus to hourly infusion ratio of 3.6 succeeded in establishing equilibrium well within 4 h in all regions. This is only a concern for high SA experiments. In low SA experiments, equilibrium is established very rapidly.

Comparison between equilibrium and kinetic analysis

There was excellent agreement between kinetic and equilibrium BP in all regions for the six experiments performed at high SA, which supported the notion that a state of equilibrium had been reached by the time of measurement of BPe. However, the standard errors associated with k_3 and k_4 were high. This was related to the absence of a washout phase, providing little information for k_4 estimation. As a result, the k_3/k_4 ratio was stable, but not their individual values. Single bolus experiments appear, thus, to be the protocol of choice for individual derivation of the rate constants.

Derivation of K_D and B_{max}

Experiments performed at low SA allowed calculation of K_D and B_{max}. As expected, B_{max} varied across regions ($p < 0.05$), but not K_D (mean K_D: 0.59 ± 0.09 n*M*). Relative regional differences in B_{max} were linearly correlated with regional differences in BP as derived by kinetic analysis of single bolus or constant infusion experiments. Provided that K_D values are not altered by disease state or medication, BP could be used as an index of receptor density.

In one animal, eight experiments were performed at various levels of SA to test the linearity of the Scatchard plot. Points were randomly distributed around the regression line and a two-site fit did not converge, indicating that [^{123}I]iomazenil was binding to a homogeneous population of sites. This confirmed the validity of the derivation of B_{max} and K_D based on results of two experiments performed at high and low SA, respectively. Additional experiments are needed to define the optimal level of receptor occupancy to be targeted with low SA experiments. If the measure variance is constant, a high receptor occupancy is desirable from the regression point of view (Rovati et al., 1988). However, reduction of counts and the statistical noise associated with very low SA must be taken into account.

Ex vivo metabolite analysis

During constant infusion experiments, the brain is exposed to high levels of metabolites for a prolonged period. It was, thus, important to verify that, under these conditions, metabolites do not significantly cross the blood–brain barrier. Metabolite levels were negligible in gray matter, indicating that the activity measured in these areas represented only parent compound.

Comparison between in vivo and in vitro results

In vivo occipital B_{max} and K_D values were in good agreement with in vitro values. In the two animals studied under in vivo and in vitro conditions, in vivo occipital B_{max} was slightly higher than for the in vitro determination (129 versus 108 n*M* for baboon 2; 137 versus 124 n*M* for baboon 3). Such divergence could be due to random variation of measurements, to systematic errors such as errors in the SPECT counts to μCi conversion factor or in vitro determination of f_1, or to a loss of receptors during tissue homogenization and washing procedures. The in vivo K_D (0.54 ± 0.04) was closer to the 37°C K_D value than to the 22°C value, suggesting that in vitro experiments performed at 37°C are more appropriate for estimating in vivo parameters than are experiments performed at nonphysiological temperatures.

As previously observed for the kinetic BP (Laruelle et al., 1994, Fig. 6), the in vivo B_{max} in frontal and temporal areas appeared to be underestimated by ~10–15% as compared to in vitro values. The in vivo B_{max} in striatum and thalamus was overestimated by 25%. We attribute these differences to the small size of the baboon's brain and to partial voluming effect (see Laruelle et al., 1994).

The in vivo k_{on} (0.025 ± 0.003 min^{-1} nM^{-1}) and k_{off} (0.015 ± 0.001 min^{-1}) values were markedly lower than were the in vitro k_{on} (0.364 ± 0.053 min^{-1} nM^{-1}) and k_{off} (0.320 ± 0.006 min^{-1}) values measured at 37°C. However, the k_{off}/k_{on} ratio was similar in vivo (0.62 ± 0.09 n*M*) and in vitro (0.84 ±

0.11 n*M*). This led to the conclusion that both the association and dissociation processes are markedly slower in vivo than in vitro. A similar observation was reported and discussed for [^{3}H]scopolamine in vivo binding in rodents (Frey et al., 1985). The authors suggested that diffusion barriers and/or competition with endogenous transmitters could explain the in vivo–in vitro discrepancy. Since we observed lower association and dissociation rates in vivo, we would favor the first hypothesis (diffusion barriers) over the second one (endogenous competition).

In vivo receptor-ligand interaction kinetics are complex as revealed by the discrepancy between the off-rate measured at tracer doses and the rapid washout induced by flumazenil injection. Similar observations have been reported with various opiate (Perry et al., 1980; Frost and Wagner, 1984) and dopamine D_2 antagonists (Votaw and Kessler, 1991). We observed the same phenomenon with the dopamine transporter ligand [^{123}I]β-CIT (Laruelle et al., 1993*c*).

To explain this phenomenon, Perry et al. (1980) and Frost and Wagner (1984) postulated the existence of a synaptic compartment in which the ligand is trapped by rebinding processes in the presence of available receptors. More formally, these theories propose that the observed dissociation rate (k_{out}) is related to the true molecular dissociation rate (k_{off}) according to

$$k_{out} = \frac{x}{x + k_{on}B_{max}'} k_{off}$$

where B_{max}' is the density of receptors available for binding. At full receptor occupancy (for example, after flumazenil injection), $B_{max}' = 0$ and $k_{out} = k_{off}$. The synaptic compartment theory in this formulation only partially explains the data reported here. This theory predicts a higher observed k_{off} (k_{out}) and a lower affinity at high receptor occupancy as compared to low receptor occupancy. In that case, the Scatchard plot would be curvilinear. However, the Scatchard plot reported here was linear, indicating that [^{123}I]iomazenil was bound to a homogenous population of sites with similar affinity at any level of receptor occupancy. Thus, the relationship between receptor occupancy and the kinetics of in vivo ligand–receptor interaction remains to be elucidated.

Conclusion

In conclusion, we demonstrated the feasibility of measuring receptor parameters B_{max} and K_D with SPECT, using equilibrium analysis of radiotracer constant infusion experiments. The accuracy of the determination of BP, K_D, and B_{max} was confirmed by in vitro binding experiments performed on the same animals. Implementation of this method in human subjects is currently under investigation.

Acknowledgment: The authors wish to thank W. Hunkeler, PhD (Hoffman-La Roche, Basle, Switzerland) for samples of iomazenil and flumazenil; E. O. Smith, G. Wisniewski, L. Pantages-Torok, and Q. Ramsby for their excellent technical assistance in collecting and analyzing the in vivo data; and S. Giddings for performing the in vitro experiments. This work was supported in part by funds from the Department of Veterans Affairs (Merit review to R. B. Innis and the Center for the Study of Posttraumatic Stress Disorder) and the Public Health Service (MHS25642 and NS06208).

REFERENCES

Beer H-F, Blauenstein PA, Hasler PH, et al. (1990) In vitro and in vivo evaluation of iodine-123 Ro 16-0154: a new imaging agent for SPECT investigations of benzodiazepine receptors. *J Nucl Med* 31:1,007–1,014

Brouillet E, Chavoix C, Khalili-Varasten M, et al. (1990) Quantitative evaluation of benzodiazepine receptors in live *Papio anubis* baboons using positron emission tomography. *Mol Pharmacol* 38:445–451

Carson RE, Channing MA, Blasberg RG, et al. (1992) Comparison of bolus and infusion methods for receptor quantification: application to [^{18}F]-cyclofoxy and positron emission tomography. *J Cereb Blood Flow Metab* 13:24–42

Dubey RK, McAllister CB, Inoue M, Wilkinson GR (1989) Plasma binding and transport of diazepam across the blood-brain barrier. No evidence for in vivo enhanced dissociation. *J Clin Invest* 84:1,155–1,159

Farde L, Eriksson L, Blomquist G, Halldin C (1989) Kinetic analysis of central [^{11}C]raclopride binding to D_2 dopamine receptors studied by PET-A comparison to the equilibrium analysis. *J Cereb Blood Flow Metab* 9:696–708

Farde L, Hall H, Ehrin E, Sedvall G (1986) Quantitative analysis of D2 dopamine receptor binding in the living human brain by PET. *Science* 231:258–261

Frey KA, Ehrenkaufer LE, Beaucage S, Agranoff BW (1985) Quantitative in vivo receptor binding I. Theory and application to the muscarinic cholinergic receptor. *J Neurosci* 5: 421–428

Frost JJ, Douglass KH, Mayberg HS, et al. (1989) Multicompartimental analysis of ^{11}C-carfentanil binding to opiate receptors in human measured by positron emission tomography. *J Cereb Blood Flow Metab* 9:398–409

Frost JJ, Wagner HN Jr. (1984) Kinetics of binding to opiate receptors in vivo predicted from in vitro parameters. *Brain Res* 305:1–11

Holman BL, Carvalho PA, Zimmerman RE, et al. (1990) Brain perfusion SPECT using an annular single crystal camera: initial clinical experience. *J Nucl Med* 31:1,456–1,461

Innis RB, Zoghbi SS, Johnson EW, Woods SW, Al-Tikriti MS, Baldwin RM, Seibyl JP, Malison RT, Zubal IG, Charney DS, Heninger GG, Hoffer PB (1991) SPECT imaging of the benzodiazepine receptor in non-human primate brain with [^{123}I]Ro 16-0154. *Eur J Pharmacol* 193:249–252

Innis RB, Al-Tikriti MS, Zoghbi SS, et al. (1991*b*) SPECT imaging of the benzodiazepine receptor: feasibility of in vivo potency measurements from stepwise displacement curves. *J Nucl Med* 32:1,654–1,761

Iyo M, Itoh T, Yamasaki T, et al. (1991) Quantitative in vivo analysis of benzodiazepine binding sites in the human brain

using positron emission tomography. *Neuropharmacology* 30:207–215

Kawai R, Carson RE, Dunn B, Newman AH, Rice KC, Blasberg RG (1991) Regional brain measurement of B_{max} and K_D with the opiate antagonist cyclofoxy: equilibrium studies in the conscious rat. *J Cereb Blood Flow Metab* 11:529–544

Koeppe RA, Holthoff VA, Frey KA, Kilbourn MR, Kuhl DE (1991) Compartmental analysis of [^{11}C]flumazenil kinetics for the estimation of ligand transport rate and receptor distribution using positron emission tomography. *J Cereb Blood Flow Metab* 11:735–744

Laruelle M, Abi-Dargham A, Rattner Z, et al. (1993*a*) SPECT measurement of benzodiazepine receptor number and affinity in primate brain: a constant infusion paradigm with [^{123}I]iomazenil. *Eur J Pharmacol* 230:119–123

Laruelle M, Al-Tikriti M, van Dyck CH, et al. (1993*b*) D-amphetamine displacement of [^{123}I]IBF equilibrium binding in primates: a new paradigm to investigate D-amphetamine induced dopamine release. *Schizophrenia Res* 9:201

Laruelle M, Baldwin RM, Malison RT, et al. (1993*c*) SPECT imaging of dopamine and serotonin transporters with [^{123}I]β-CIT: pharmacological characterization of brain uptake in nonhuman primates. *Synapse* 13:295–309

Laruelle M, Baldwin RM, Rattner Z, Al-Tikriti MS, Zea-Ponce Y, Zoghbi SS, Charney DS, Price JC, Frost JJ, Hoffer PB, Innis RB (1994) SPECT quantification of [^{123}I]iomazenil binding to benzodiazepine receptors in nonhuman primates: I. kinetic modeling of single bolus experiments. *J Cereb Blood Flow Metab* 14:439–452

Logan J, Wolf AP, Shiue CY, Fowler JS (1987) Kinetic modeling of receptor-ligand binding applied to positron emission tomographic studies with neuroleptic tracers. *J Neurochem* 48:73–83

Mintun MA, Raichle ME, Kilbourn MR, Wooten GF, Welch MJ (1984) A quantitative model for the in vivo assessment of drug binding sites with positron emission tomography. *Ann Neurol* 15:217–227

Munson P, Rodbard D (1980) LIGAND: A versatile computerized approach for characterization of ligand binding systems. *Ann Biochem* 107:220–239

Pappata S, Samson Y, Chavoix C, Prenant C, Maziere M, Baron JC (1988) Regional specific binding of [^{11}C]Ro 15-1788 to central type benzodiazepine receptors in human brain: quantitative evaluation by PET. *J Cereb Blood Flow Metab* 8: 304–313

Perry DC, Mullis KB, Øie S, Sadee W (1980) Opiate antagonist receptor binding in vivo: evidence for a new receptor binding model. *Brain Res* 199:49–61

Rovati GE, Rodbard DE, Munson PJ (1988) DESIGN: Computerized optimization of experimental design for estimating Kd and Bmax in ligand binding experiments. *Ann Biochem* 174: 636–649

Scatchard G (1949) The attraction of proteins for small molecules and ions. *Ann NY Acad Sci* 51:660–672

Sybirska E, Al-Tikriti M, Zoghbi SS, Baldwin RM, Johnson EW, Innis RB (1992) SPECT imaging of the benzodiazepine receptor: autoradiographic comparison of receptor density and radioligand distribution. *Synapse* 12:119–128

Votaw JR, Kessler RM (1991) The effect on binding kinetics of the diffusion of neuroreceptor ligand into the synapse. *J Nucl Med* 32:1008

Zea-Ponce Y, Baldwin R, Zoghbi SS, Innis RB (1994) Formation of 1-[^{123}I]iodobutane in iododestannylation with [^{123}I]iomazenil: implication for the reaction mechanism. *Appl Radiat Isot* 45:63–68

Zoghbi SS, Baldwin RM, Seibyl JP, et al. (1992) Pharmacokinetics of the SPECT benzodiazepine receptor radioligand [^{123}I]iomazenil in human and nonhuman primates. *Nucl Med Biol* 19:881–888